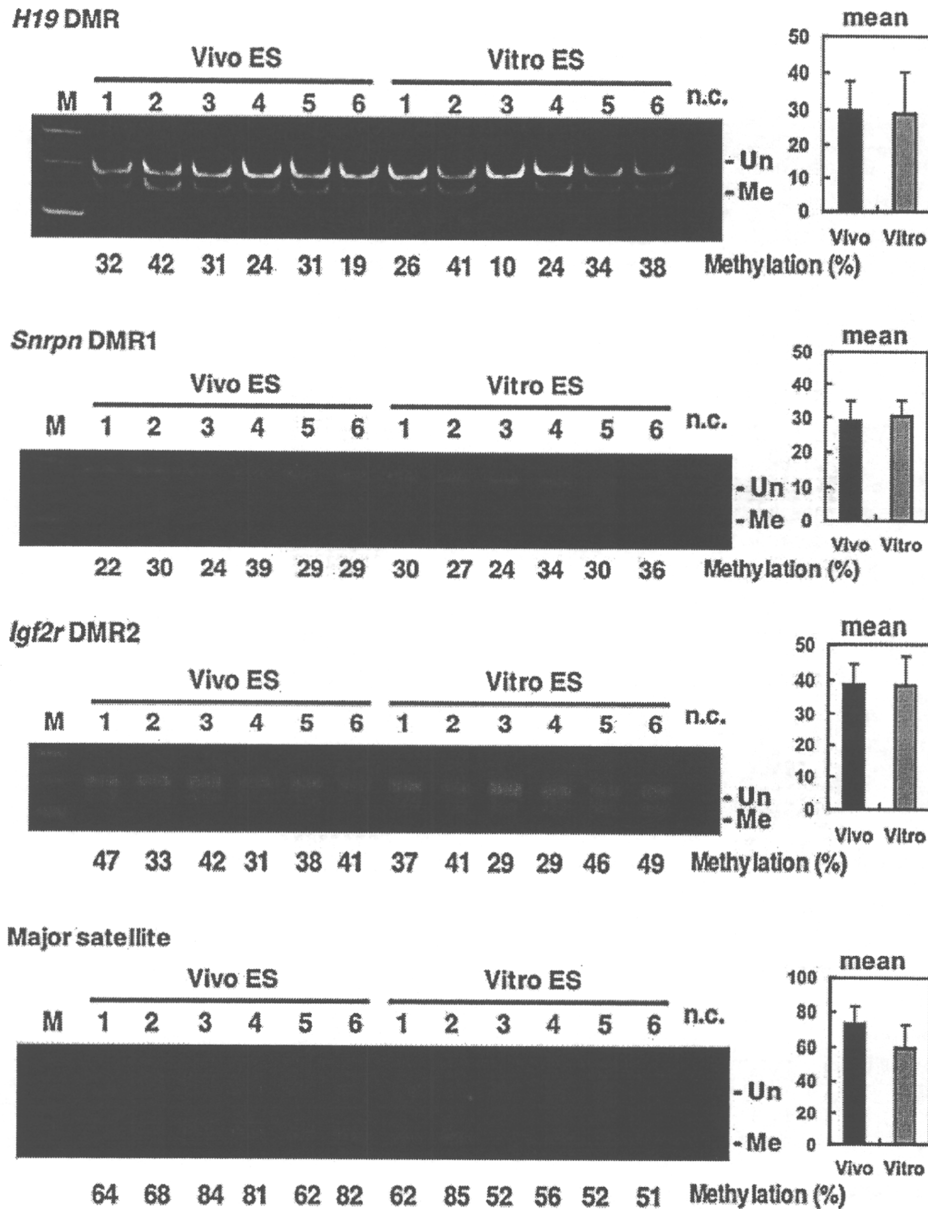

FIG. 7. Methylation status of imprinted genes and satellite repeats at later passages (passage 5) in Vivo and Vitro ES cells (BPF1 mouse strain). There was no significant difference in the percentage of methylated sites for either ES cell line. M: marker, n.c: negative control, Un: unmethylated, Me: methylated.

normal imprinting can be easily disrupted during preimplantation development *in vitro*. For example, *in vitro* cultured blastocysts often exhibit hypomethylation of the *H19* DMR, which results in the biallelic expression of the *H19* gene (Doherty et al., 2000; Mann et al., 2004; Sasaki et al., 1995). In our study, abnormal imprinting was still observed in early-passage Vitro ES cells. According to the expression analysis at this time point, *Dnmt3b* mRNA expression levels were significantly lower in Vitro ES cells than in Vivo ES cells. Dnmt3b is well known as a *de novo* methyltransferase, and is required for the establishment of new methylation patterns during embryonic development (Okano et al., 1999). Dnmt3b is also required for the maintenance of DNA methylation in addition to the major maintenance methyltransferase Dnmt1 (Dodge et al., 2005). These reports suggest that low expression levels of Dnmt3b may result in unstable genomic imprinting in Vitro ES cells.

In addition, hypomethylation in XX ES cells is associated with reduced levels of Dnmt3a and Dnmt3b, and it is known that the ectopic expression of these factors restores global methylation levels (Zvetkova et al., 2005), which supports our hypothesis. However, the demethylation of the *H19*

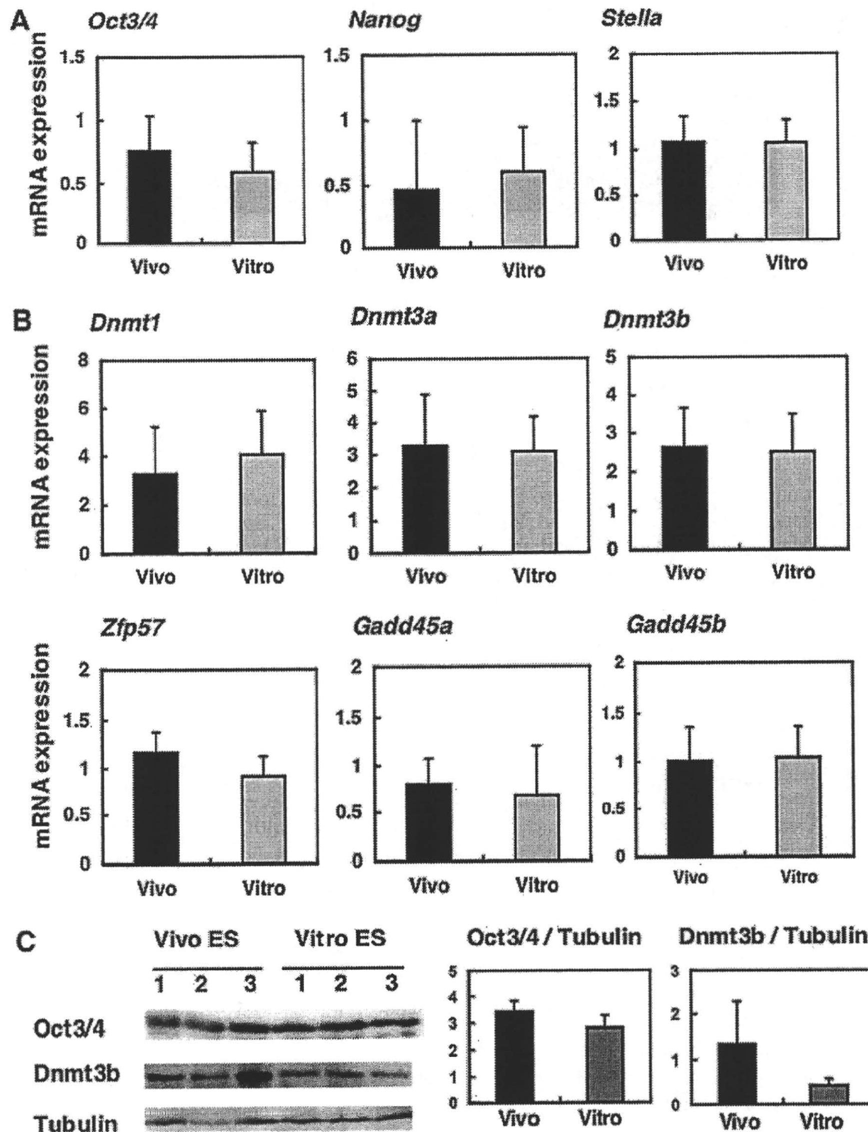

FIG. 8. Expression patterns of Vivo and Vitro ES cells (BPF1 mouse strain) at later passages (passage 6: V1–V4 and Vt1–Vt4, passage 5: V5, V6, Vt5, and Vt6). (**A**) Quantitative real-time PCR analysis for ES cell markers (*Oct3/4*, *Nanog*, and *Stella*). (**B**) Quantitative real-time PCR analysis for three DNA methyltransferases (*Dnmt1*, *Dnmt3a*, and *Dnmt3b*), and three putative methylation-related genes (*Zfp57*, *Gadd45a*, and *Gadd45b*). Data are the means ± standard deviations ($n = 6$). (**C**) Immunoblot analysis with anti-Oct3/4 and anti-Dnmt3b. Anti-α-tubulin was used for normalizing the data. Data are the means ± standard deviations.

DMR was observed not only in XX ES cells but also in XY ES cells in our study (Fig. 6), indicating that other factors are also involved in demethylation. For example, *Gadd45b*, reported as a putative demethylation factor, was more highly expressed in Vitro ES cells than Vivo ES cells in the BPF1 mouse strain. *Gadd45* genes have been implicated in stress signaling in response to physiological or environmental stress factors, such as activated oxygen species, X-rays, and UV radiation (Liebermann and Hoffmann, 2008); therefore, *in vitro* culture conditions, which differ from the environments of the oviduct and uterus, could induce stress signaling and result in the upregulation of *Gadd45* mRNA expression, possibly promoting disruption of normal imprinting. In contrast, the expression levels of *Stella* and *Zfp57* genes were not different in BPF1 ES cells. Although B6 ES cell lines showed significant differences in *Zfp57* expression, this gene is not associated with *H19* demethylation (Li et al., 2008). The shift in gene expression patterns of several methylation related-genes seems to promote demethylation and to inhibit methylation in early passage Vitro ES cells. On the other hand, immunoblot analysis did not detect differences in Dnmt3b expression levels, suggesting that Dnmt3b is unrelated to the epigenetic instability of Vitro ES cells and that other factors are involved in demethylation.

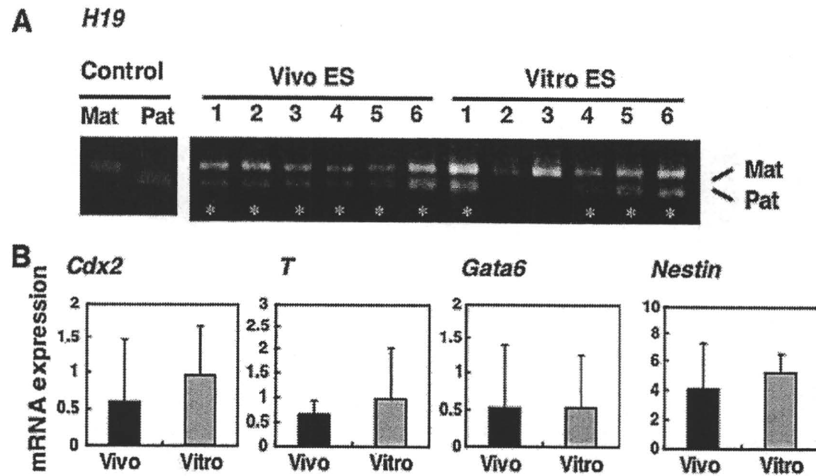

FIG. 9. Gene expression patterns of Vivo and Vitro ES cell-derived EBs (BPF1 mouse strain). (**A**) Allelic expression patterns of the *H19* imprinted gene in individual Vivo and Vitro ES cell-derived EBs. Both Vivo and Vitro ES cells often display biallelic expression (*). Mat: maternal allele (B6), Pat: paternal allele (PWK). (**B**) Quantitative real-time PCR analysis for genes expressed in each of the three germ layers, *Cdx2* (trophectoderm), *T* (mesoderm), *Gata6* (primitive endoderm), and *Nestin* (neural progenitor). Significant differences in differentiation ability were not observed between Vivo and Vitro ES cells. Data are the means $\pm$ standard deviations ($n = 6$).

In any case, we observed several differences in methylation status and mRNA expression patterns between Vivo and Vitro ES cells at very early passages, but no significant differences were found at later passages. Long-term culture of ES cells often affects the methylation status of imprinted genes and their totipotency (Dean et al., 1998). In our study, obviously abnormal genomic imprinting appears in both Vivo and Vitro ES cell lines at passage 5. The *H19* gene shows monoallelic expression in normal embryos (Mann et al., 2004); however, biallelic expression of this gene was observed at later passages of both types of ES cell line. We generated EBs to elucidate the pluripotency of Vitro ES cells, but we found no significant differences between Vivo and Vitro ES cells.

Our study has clarified that Vivo ES cells exhibited a more normal epigenotype than Vitro ES cells only at very early passages (below passage 2). In contrast, there was no significant difference between Vivo and Vitro ES cells at later passages. Therefore, we have to consider that repeated passages of ES cells disrupt normal genomic imprinting, leading to the abnormal biallelic expression of imprinted genes. Epigenetic alterations that arise after establishment and culture of ES cell lines are not corrected during postimplantation development, and these alterations are associated with aberrant imprinted gene expression in the fetus (Dean et al., 1998). In conclusion, it is advisable to use early-passage Vivo ES cells whenever possible to avoid abnormalities caused by long-term culture in mice. On the other hand, because Vitro ES cells are the only ones available in humans, a careful selection of ES cell lines is necessary to avoid the aberrant expression of imprinted genes, which could lead to abnormal development and disease.

Acknowledgments

We thank Dr. Tsukasa Oda (Gunma University) and Tomoyuki Tsukiyama (Kyoto University) for technical advice on immunoblot analysis, and Dr. Shoji Tajima (Osaka University) for providing the anti-Dnmt3b antibody. This work was supported in part by grants from the Japan Society for the promotion of Science (JSPS; 17770182); the Japan Science and Technology Corporation (JST); the Ministry of Education, Culture, Sports, Science and Technology of Japan; the Ministry of Health, Labour and Welfare of Japan; the Japan Health Sciences Foundation; and the National Institute of Biomedical Innovation.

Author Disclosure Statement

The authors declare that no conflicting financial interests exist.

References

Barreto, G., Schafer, A., Marhold, J., et al. (2007). Gadd45a promotes epigenetic gene activation by repair-mediated DNA demethylation. Nature 445, 671–675.

Bartolomei, M.S., Zemel, S., and Tilghman, S.M. (1991). Parental imprinting of mouse *H19* gene. Nature 351, 153–155.

Buehr, M., and McLaren, A. (1993). *Guide to Techniques in Mouse Development.* (Academic Press, San Diego, CA), pp. 58–77.

Cox, G.F., Burger, J., Lip, V., et al. (2002). Intracytoplasmic sperm injection may increase the risk of imprinting defects. Am. J. Hum. Genet. 71, 162–164.

Dean, W., Bowden, L., Aitchison, A., et al. (1998). Altered imprinted gene methylation and expression in completely ES cell-derived mouse fetuses: association with aberrant phenotypes. Development 125, 2273–2282.

DeBaun, M.R., Niemitz, E.L., and Feinberg, A.P. (2003). Association of in vitro fertilization with Beckwith-Wiedemann syndrome and epigenetic alterations of LIT1 and H19. Am. J. Hum. Genet. 72, 156–160.

Dodge, J.E., Okano, M., Dick, F., et al. (2005). Inactivation of Dnmt3b in mouse embryonic fibroblasts results in DNA hypomethylation, chromosomal instability, and spontaneous immortalization. J. Biol. Chem. 280, 17986–17991.

Doetschman, T.C., Eistetter, H., Katz, M., et al. (1985). The in vitro development of blastocyst-derived embryonic stem cell lines: formation of visceral yolk sac, blood islands and myocardium. J. Embryol. Exp. Morphol. 87, 27–45.

Doherty, A.S., Mann, M.R.W., Tremblay, K.D., et al. (2000). Differential effects of culture on imprinted *H19* expression in the preimplantation mouse embryo. Biol. Reprod. 62, 1526–1535.

Evans, M.J., and Kaufman, M.H. (1981). Establishment in culture of pluripotential cells from mouse embryos. Nature 292, 154–156.

Ferguson-Smith, A.S., Cattanach, B.M., Barton, S.C., et al. (1991). Embryological and molecular investigations of parental imprinting on mouse chromosome 7. Nature 351, 667–670.

Fournier, C., Goto, Y., Ballestar, E., et al. (2002). Allele-specific histone lysine methylation marks regulatory regions at imprinted mouse genes. EMBO J. 21, 6560–6570.

Gicquel, C., Gaston, V., Mandelbaum, J., et al. (2003). In vitro fertilization may increase the risk of Beckwith-Wiedemann syndrome related to the abnormal imprinting of the KCN1OT gene. Am. J. Hum. Genet. 72, 1338–1341.

Horii, T., Nagao, Y., Tokunaga, T., et al. (2003). Serum-free culture of murine primordial germ cells and embryonic germ cells. Theriogenology 59, 1257–1264.

Horii, T., Kimura, M., Morita, S., et al. (2008). Loss of genomic imprinting in mouse parthenogenetic embryonic stem cells. Stem Cells 26, 79–88.

Kim, J.M., and Ogura, A. (2009). Changes in allele-specific association of histone modifications at the imprinting control regions during mouse preimplantation development. Genesis 47, 611–616.

Kobayashi, H., Suda, C., Abe, T., et al. (2006). Bisulfite sequencing and dinucleotide content analysis of 15 imprinted mouse differentially methylated regions (DMRs): paternally methylated DMRs contain less CpGs than maternally methylated DMRs. Cytogenet. Genome Res. 113, 130–137.

Kumaki, Y., Oda, M., and Okano, M. (2008). QUMA: quantification tool for methylation analysis. Nucleic Acids Res. 36, W170–W175.

Li, E., Bestor, T.H., and Jaenisch, R. (1992). Targeted mutation of the DNA methyltransferase gene results in embryonic lethality. Cell 69, 915–926.

Li, X., Ito, M., Zhou, F., et al. (2008). A maternal-zygotic effect gene, Zfp57, maintains both maternal and paternal imprints. Dev. Cell 15, 547–557.

Liebermann, D.A., and Hoffman, B. (2008). Gadd45 in stress signaling. J. Mol. Signal. 3, 15.

Ma, D.K., Jang, M.H., Guo, J.U., et al. (2009). Neuronal activity-induced Gadd45b promotes epigenetic DNA demethylation and adult neurogenesis. Science 323, 1074–1077.

Maher, E.R., Brueton, L.A., Bowdin, S.C., et al. (2003) Beckwith-Wiedemann syndrome and assisted reproduction technology (ART). J. Med. Genet. 40, 62–64.

Mann, M.R., Lee, S.S., Doherty, A.S., et al. (2004). Selective loss of imprinting in the placenta following preimplantation development in culture. Development 131, 3727–3735.

Martin, G.R. (1975). Teratocarcinomas as a model system for the study of embryogenesis and neoplasia. Cell 5, 229–243.

Martin, G.R. (1981). Isolation of a pluripotent cell line from early mouse embryos cultured in medium conditioned by teratocarcinoma stem cells. Proc. Natl. Acad. Sci. USA 78, 7634–7638.

Morita, S., Horii, T., Kimura, M., et al. (2007). One Argonaute family member, Eif2c2 (Ago2), is essential for development and appears not to be involved in DNA methylation. Genomics 89, 687–696.

Murry, C.E., and Keller, G. (2008). Differentiation of embryonic stem cells to clinically relevant populations: lessons from embryonic development. Cell 132, 661–680.

Nakamura, T., Arai, Y., Umehara, H., et al. (2007). PGC7/Stella protects against DNA demethylation in early embryogenesis. Nat. Cell Biol. 9, 64–71.

Okano, M., Xie, S., and Li, E. (1998). Cloning and characterization of a family of novel mammalian DNA (cytosine-5) methyltransferases. Nat. Genet. 19, 219–220.

Okano, M., Bell, D.W. Haber, D.A., et al. (1999). DNA methyltransferases Dnmt3a and Dnmt3b are essential for de novo methylation and mammalian development. Cell 99, 247–257.

Orstavik, K.H., Eiklid, K., van der Hagen, C.B., et al. (2003). Another case of imprinting defect in a girl with Angelman syndrome who was conceived by intracytoplasmic semen injection. Am. J. Hum. Genet. 72, 218–219.

Pfeifer, K. (2000). Mechanisms of genomic imprinting. Am. J. Hum. Genet. 67, 777–787.

Robertson, E.J. (1987). Embryo derived stem cell lines. In *Teratocarcinomas and Embryonic Stem Cells: A Practical Approach.* E.J. Robertson, ed. (IRL Press, Oxford) pp. 71–112.

Sasaki, H., Ferguson-Smith, A.C., Shum, A.S.W., et al. (1995). Temporal and spatial regulation of *H19*imprinting in normal and uniparental mouse embryos. Development 121, 4195–4202.

Stevens, L.C. (1975). Comparative development of normal and parthenogenetic mouse embryos, early testicular and ovarian teratomas and embryoid bodies. In *Teratomas and Differentiation.* M.I. Sherman and D. Solter, eds. (Academic Press, New York) pp. 17–32.

Szabo, P.E., and Mann, J.R. (1995). Biallelic expression of imprinted genes in the mouse germ line: implications for erasure, establishment, and mechanisms of genomic imprinting. Genes Dev. 9, 1857–1868.

Tielens, S., Verhasselt, B., Liu, J., et al. (2006). Generation of embryonic stem cell lines from mouse blastocysts developed in vivo and in vitro: relation to Oct-4 expression. Reproduction 132, 59–66.

Toyoda, Y., Yokoyama, M., and Hoshi, T. (1971). Studies on the fertilization of mouse eggs in vitro: I. In vitro fertilization of eggs by fresh epididymal sperm. Jpn. J. Anim. Reprod. 16, 147–151.

Xiong, Z., and Laird, P.W. (1997). COBRA: a sensitive and quantitative DNA methylation assay. Nucleic Acids Res. 25, 2532–2534.

Yamasaki, Y., Kayashima, T., Soejima, H., et al. (2005). Neuron-specific relaxation of Igf2r imprinting is associated with neuron-specific histone modifications and lack of its antisense transcript Air. Hum. Mol. Genet. 14, 2511–2520.

Zvetkova, I., Apedaile, A., Ramsahoye, et al. (2005). Global hypomethylation of the genome in XX embryonic stem cells. Nat. Genet. 37, 1274–1279.

Address correspondence to:
Dr. Izuho Hatada
Laboratory of Genome Science
Biosignal Genome Resource Center Institute
for Molecular and Cellular Regulation
Gunma University
3-39-15 Showa-machi
Maebashi, Gunma 371-8512, Japan

E-mail: ihatada@showa.gunma-u.ac.jp

Ando et al. BMC Molecular Biology 2011, 12:6
http://www.biomedcentral.com/1471-2199/12/6

BMC Molecular Biology

RESEARCH ARTICLE Open Access

Two-step cleavage of hairpin RNA with 5' overhangs by human DICER

Yoshinari Ando[1], Yoshiko Maida[2], Ayako Morinaga[1], Alexander M Burroughs[1], Ryuichiro Kimura[3], Joe Chiba[3], Harukazu Suzuki[1], Kenkichi Masutomi[2,4], Yoshihide Hayashizaki[1*]

Abstract

Background: DICER is an RNase III family endoribonuclease that processes precursor microRNAs (pre-miRNAs) and long double-stranded RNAs, generating microRNA (miRNA) duplexes and short interfering RNA duplexes with 20~23 nucleotides (nts) in length. The typical form of pre-miRNA processed by the Drosha protein is a hairpin RNA with 2-nt 3' overhangs. On the other hand, production of mature miRNA from an endogenous hairpin RNA with 5' overhangs has also been reported, although the mechanism for this process is unknown.

Results: In this study, we show that human recombinant DICER protein (rDICER) processes a hairpin RNA with 5' overhangs *in vitro* and generates an intermediate duplex with a 29 nt-5' strand and a 23 nt-3' strand, which was eventually cleaved into a canonical miRNA duplex via a two-step cleavage. The previously identified endogenous pre-miRNA with 5' overhangs, pre-mmu-mir-1982 RNA, is also determined to be a substrate of rDICER through the same two-step cleavage.

Conclusions: The two-step cleavage of a hairpin RNA with 5' overhangs shows that DICER releases double-stranded RNAs after the first cleavage and binds them again in the inverse direction for a second cleavage. These findings have implications for how DICER may be able to interact with or process differing precursor structures.

Background

DICER plays a key role in RNA interference pathways through the biogenesis of microRNA (miRNA) and small interfering RNA (siRNA) [1-3]. Most miRNA genes are transcribed as long primary transcripts (pri-miRNAs) where stem-loop structures with mature miRNA sequences embedded in the arm of a stem are cleaved by the Drosha nuclear microprocessor complex releasing a precursor miRNA (pre-miRNA) hairpin [4,5]. The cleavage site is determined mainly by the distance (~11 bp) from the stem-single stranded RNA junction of pri-miRNA and most pre-miRNAs have 2 nt-3' overhangs [6]. Pre-miRNAs, exported into the cytoplasm by Exportin-5 and Ran-GTP [7], are processed by the RISC loading complex (RLC) into 20~23 nt duplexes where the RNase III enzyme DICER plays a central role together with the double stranded (ds) RNA-binding proteins TRBP and PACT and the miRNA-associated RNA-induced silencing complex (miRISC) core component Argonaute-2 (AGO2) [8-10]. miRNA duplexes processed by RLC are finally loaded to miRISC as a double stranded-structure [11] and separated into the functional guide strand, which is complementary to the target, and the passenger strand, which is subsequently degraded [12,13]. Strand selection of the functional guide strand by AGO2 depends on the thermodynamic stabilities of the base pairs at the 5' ends of the two strands [12,14,15]. Duplexes of siRNA or miRNA produced by DICER can be loaded in either direction to Argonaute [16-18]. Indeed, the mature miRNA either in the 5' or 3' strands can be harboured from pre-miRNA [19-21]. On the other hand, endogenous human AGO2 can bind directly to pre-miRNAs in DICER-knockout cells [22]. Recently, it was reported that human DICER is not essential for loading dsRNAs to AGO2 but functions in pre-selection of effective siRNAs for handoff to AGO2 [23].

Human DICER is a ~220 kDa protein consisting of several domains; an N-terminal DExH-box RNA helicase-like domain, a DUF283 domain, a PAZ domain,

* Correspondence: yosihide@gsc.riken.jp
[1]RIKEN Omics Science Center, 1-7-22 Suehiro-cho, Tsurumi-ku, Yokohama 230-0045, Japan
Full list of author information is available at the end of the article

BioMed Central

© 2011 Ando et al; licensee BioMed Central Ltd. This is an Open Access article distributed under the terms of the Creative Commons Attribution License (http://creativecommons.org/licenses/by/2.0), which permits unrestricted use, distribution, and reproduction in any medium, provided the original work is properly cited.

two RNase III domains (RIIIa and RIIIb), and a dsRNA binding motif domain (DARM) [24]. The two RNase III domains of DICER form a single dsRNA processing center via intramolecular dimerization which together cleave the opposite strands of the dsRNA, generating dinucleotide-long 3' overhangs on both ends [25]. The crystal structure of Dicer from *Giardia intestinalis* showed that the hydrophobic pocket of the PAZ domain was responsible for the binding of the 3' dinucleotide overhangs of the substrate and the connector helix between the PAZ domain and RNase III domain functioned as a molecular ruler measuring the distance from the 3' end of pre-miRNA to the cleavage site [26,27]. However, 3'-dinucleotide dsRNA overhangs are not essential for binding with DICER [28]. When the 3' overhang is removed, DICER can still cleave dsRNA through interaction with the remaining 5' overhang [28]. This is consistent with MacRae *et al.* who found that the recombinant Dicer protein of *Giardia intestinalis* could cleave the dsRNA with 5' overhangs [27]. However, they used perfectly matched dsRNAs with no gap, which might resemble an endogenous siRNA precursor. An additional study by Flores-Jasso *et al.* showed that human recombinant DICER protein could nick either strand of a mononucleotide-5' overhanged pre-miRNA with some strand preferences [29]. Despite this, the detailed step mechanism for pre-miRNA cleavage, especially for the pre-miRNA with 5' overhangs, is not yet elucidated.

An alternative nuclear pathway of pre-miRNA biogenesis was described where a short intron with a hairpin can be spliced and debranched into pre-miRNA hairpin mimics (mirtrons) [30-32]. This processing pathway uses intron splicing machinery instead of the Drosha endonuclease; miRNA precursors generated from intronic sequences (debranched mirtrons) are believed to be incorporated into the canonical miRNA pathway as a substrate of DICER. Interestingly, mouse pre-mir-1982 is a mirtron with an 11 nt tail at the 5' end [33], although most mammalian mirtron are hairpin structures with single nucleotide overhangs at both ends [32-34]. Mature mouse miR-1982* miRNA emerges without 11 nt-5' overhangs from deep sequencing data of murine cells [33,35] while the elimination mechanism of this 11 nt-5' tail is still unknown.

In this paper, we investigated the detailed processing pattern of hairpin RNAs containing 5' overhangs by human recombinant DICER. We show here that human recombinant DICER is able to process hairpin RNA with 5' overhangs and two-step cleavage by DICER forms the mature miRNA duplex from the hairpin RNAs. Additionally, pre-mmu-mir-1982 RNA, which is a natural hairpin RNA with 5' overhangs, is also processed by a two-step cleavage mediated by human recombinant DICER protein *in vitro*.

Results and Discussion

Processing of the pre-miRNA by recombinant DICER protein

We prepared purified recombinant DICER1 (rDICER) protein containing a FLAG-tag at the N-terminus (see Figures 1A and 1B). This rDICER does not contain known DICER-binding partners, AGO2 and TRBP (see Figure 1C). In order to confirm activity, we attempted to cleave pre-miRNA hairpin RNA using the rDICER. Forty-five pmol of pre-mir-21 RNA (see Figure 2A) was incubated with 2 pmol of the purified rDICER at the indicated times followed by purification. The reacted RNA substrates were subjected to Northern blotting using probe-1, corresponding to the antisense sequence of bases 2-22 of pre-mir-21 (see Figure 2A). A single band, 23 nucleotides in length, appeared after 20 min incubation and gradually increased. Thus, the purified rDICER possessed reasonable pre-miRNA processing activity to produce ~23 nt mature miRNA *in vitro* (see Figure 2B).

Processing of the hairpin RNA with 5' overhangs, RNA-I, by recombinant DICER protein

Using this rDICER, we performed a cleavage assay on a designed pre-miRNA mimic of hairpin RNA with trinucleotide-5' overhangs (RNA-I, see Figure 3A) to analyze whether DICER could process a hairpin RNA with 5' overhangs. The cleavage products were detected by Northern blotting using three different probes, probe-1, probe-2 and probe-3, corresponding to antisense

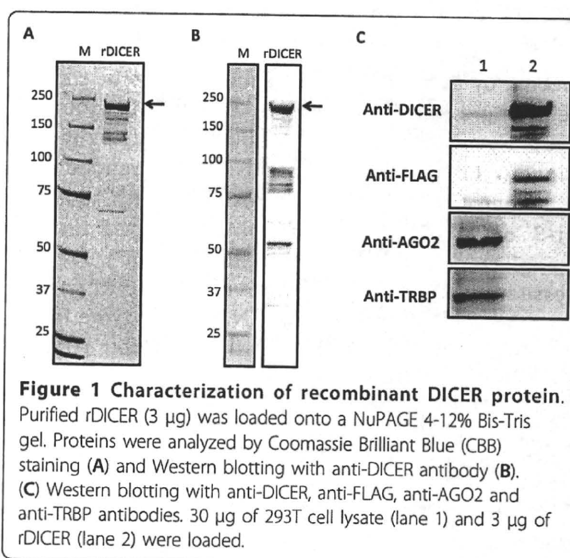

Figure 1 Characterization of recombinant DICER protein. Purified rDICER (3 μg) was loaded onto a NuPAGE 4-12% Bis-Tris gel. Proteins were analyzed by Coomassie Brilliant Blue (CBB) staining (**A**) and Western blotting with anti-DICER antibody (**B**). (**C**) Western blotting with anti-DICER, anti-FLAG, anti-AGO2 and anti-TRBP antibodies. 30 μg of 293T cell lysate (lane 1) and 3 μg of rDICER (lane 2) were loaded.

Figure 2 Processing of the precursor miRNA by recombinant DICER protein. (**A**) Precursor miRNA (pre-mir-21 RNA) and probe used in this study. The 5' end nucleotide of pre-mir-21 RNA was modified (U to G) from human pre-hsa-mir-21 RNA sequence registered in miRBase 14.0 [46-48] in order to facilitate the *in vitro* transcription reaction. The secondary structure was predicted using the CentroidFold program [49]. The solid line shows the position of probe-1. (**B**) Detection of the rDICER-processed products by Northern blotting. Pre-mir-21 RNAs were incubated with rDICER *in vitro* for the indicated time points (0, 10, 20, 30, 40, 50, 60, 75, 90, 105 and 120 min). The RNAs processed by rDICER were detected using probe-1 by Northern blotting. The gray arrow shows the band of pre-mir-21 RNA and the black arrow shows the band of miRNA processed from the 5' strand of pre-mir-21 RNA. The asterisk shows the nicked product (~37 nt) similar to a previous report [29].

sequences of bases 11-32, bases 49-69 and bases 33-48 of RNA-I, respectively (see Figure 3A). Using probe-1, band 1 (~30nt) appeared after 20 min incubation and gradually increased through a 50 min-incubation. This processing pattern was similar to that of the around 23-nt product generated from native pre-miRNA by rDICER (see Figures 2B and 3B). After 40 min incubation, band 2 (~23nt) was detected and the abundance of band 2 increased in a time-dependent manner (see Figure 3B). Additionally, using probe-2, band 3 (~23nt) was detected from the 30-min incubation sample (see Figure 3C). Using probe-3, band 4 (~22nt) was detected from the 20-min incubation sample (see Figure 3D). The processing activity on the hairpin RNA with 5' overhangs is comparable to that for natural pre-miRNA. This means that hairpin RNA with 5' overhangs could also be a substrate for rDICER processing.

To analyze band 1 at a longer incubation time, the RNA-I was incubated with the purified rDICER and the cleavage reactions were performed for 30 min and 16 hours. Surprisingly, band 1 was detected at 30 min incubation but disappeared after 16-hours incubation. On the other hand, band 2 continued to accumulate (see Figure 3E). These results showed that band 1, which seems to be a product of first processing by rDICER, disappeared following an extended incubation time.

Next, to verify the size of the cleavage products of RNA-I, we cloned the 23-nt products after 16-hour rDICER incubation and sequenced them (see Table 1). Several clones were obtained from 5'-strand, 3' strand and loop region of RNA-I corresponding to bands 2-4 in Figure 3, respectively. The miRNA length heterogeneity generated by rDICER is consistent with the finding in the previous report [36]. Clones from the 5' strand lacking 6 or 7 nt the initial of the 5' end of RNA-I and clones from 3' strand lack the terminal 1 or 2 nt of the 3' end of RNA-I.

To analyze how band 1 is further processed, we labelled the 5' end of the RNA-I and incubated the samples with rDICER (see Figure 4A). Time course experiments and cloning results indicated that rDICER could process the 5'-labelled RNA-I at the 29-nt position from its 5' end (band 1) after 20 min incubation and subsequently cleave the 29-nt short RNA at the 6-nt position from its 5' end to 23-nt RNA (band 2) after 40 min incubation (see Figure 4A, 4B, and Table 1). This suggests dsRNAs with a 29 nt-5' strand and a 23 nt-3' strand are processed by rDICER from RNA-I at the first cleavage and released once from the enzyme. After this, rDICER binds the dsRNA again and, measuring from the 3' end of the 29-nt strand, generates 23-22 nt RNA duplexes via a second cleavage reaction (see Figure 5).

In this research, we found that hairpin RNA with trinucleotide-5' overhangs was cleaved into a 23-22 nt RNA duplex through two-step processing by rDICER. This could not be detected if we used only end-labelled RNA or label-incorporated RNA as a substrate for rDICER as reported previously [27,29]. In the first step, rDICER processes the hairpin RNA with 5' overhangs to dsRNA with 29 nt and 23 nt. Our results indicate the first processed dsRNA binds again in the inverse direction with the same or a different rDICER molecule and is again effective cleaved. The results are consistent with the previous report that human DICER protein binds either 3' ends of dsRNA strand on the PAZ domain and cleaves dsRNA at the ~23 nt position from the binding end [25]. In the sequential process described here, dsRNAs with 29 nt and 23 nt gradually increased and then stabilized at a steady level, followed by rapid increase of 23-22 nt duplexes (see Figure 3B and 3C). This indicates that dsRNAs with 29 nt and 23 nt are

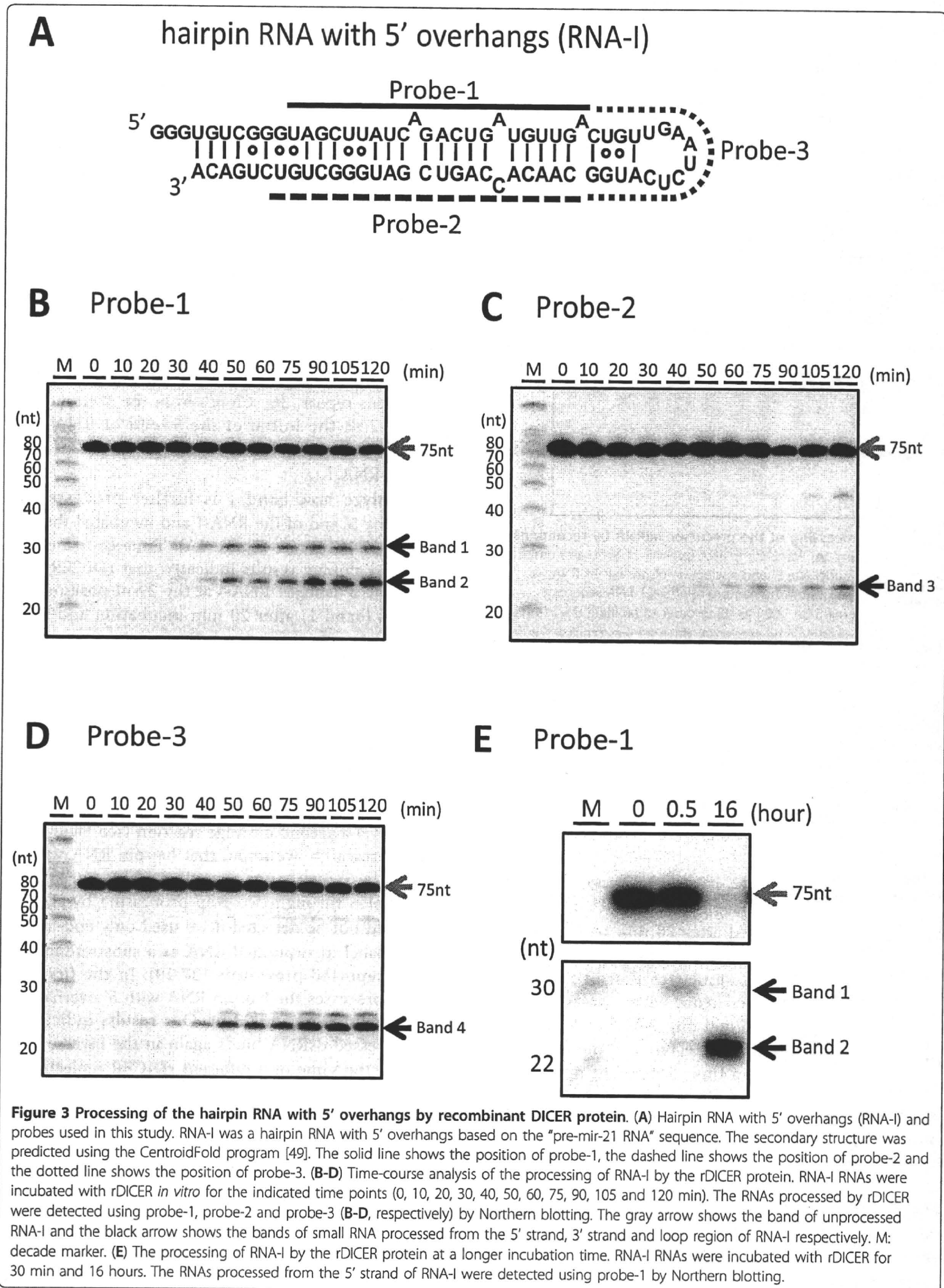

Figure 3 Processing of the hairpin RNA with 5′ overhangs by recombinant DICER protein. (**A**) Hairpin RNA with 5′ overhangs (RNA-I) and probes used in this study. RNA-I was a hairpin RNA with 5′ overhangs based on the "pre-mir-21 RNA" sequence. The secondary structure was predicted using the CentroidFold program [49]. The solid line shows the position of probe-1, the dashed line shows the position of probe-2 and the dotted line shows the position of probe-3. (**B-D**) Time-course analysis of the processing of RNA-I by the rDICER protein. RNA-I RNAs were incubated with rDICER *in vitro* for the indicated time points (0, 10, 20, 30, 40, 50, 60, 75, 90, 105 and 120 min). The RNAs processed by rDICER were detected using probe-1, probe-2 and probe-3 (**B-D**, respectively) by Northern blotting. The gray arrow shows the band of unprocessed RNA-I and the black arrow shows the bands of small RNA processed from the 5′ strand, 3′ strand and loop region of RNA-I respectively. M: decade marker. (**E**) The processing of RNA-I by the rDICER protein at a longer incubation time. RNA-I RNAs were incubated with rDICER for 30 min and 16 hours. The RNAs processed from the 5′ strand of RNA-I were detected using probe-1 by Northern blotting.

Table 1 Cloning of products from RNA-I processed by recombinant DICER protein

	Count
......CGGGUAGCUUAUCAGACUGAUGU..	23
.......GGGUAGCUUAUCAGACUGAUGU..	19
......CGGGUAGCUUAUCAGACUGAUG...	9
.....UCGGGUAGCUUAUCAGACUGAUGU..	1
.....UCGGGUAGCUUAUCAGACUGAUG...	1
.......GGGUAGCUUAUCAGACUGAUGUU...	1
......CGGGUAGCUUAUCAGACUGA...	1
.............................UGACUGUUGAAUCUCAUGGCAA........................	4
.............................UGACUGUUGAAUCUCAUGGCAACA......................	2
............................UUGACUGUUGAAUCUCAUGGCAAC.......................	1
....ACCAGUCGAUGGGCUGUCUGAC.	2
....CCAGUCGAUGGGCUGUCUGA..	2
....ACCAGUCGAUGGGCUGUCUGA..	1
GGGUGUCGGGUAGCUUAUCAGACUGAUGUUGACUGUUGAAUCUCAUGGCAACACCAGUCGAUGGGCUGUCUGACA	
...((((((((((((((((.(((((.(((((.((((........))))))))).)))))))))))))))))))))	(-34.60)

processed at a constant rate and 23-22 nt duplexes are belatedly processed at a similar rate. This suggests that the binding and processing of miRNA duplexes and releasing of the duplex from rDICER occur at the same rate. The bidirectional binding of processed dsRNA by DICER could result in directional presentation of dsRNA to Argonaute [16-18].

The effect of 5' overhangs in substrate cleavage by recombinant DICER protein

We generated three different hairpin RNAs based on pre-hsa-mir-21 RNA: pre-mir-21 RNA, RNA-I and RNA-II (see Figure 2A, 3A and Additional file 1: Figure S1A, respectively). RNA-II is the same as pre-mir-21 RNA except for 5' addition. Using probe-1 to detect the cleavage product from the 5' strand for Northern blotting, both bands of mature miRNA in Figure 2B and band 1 (first cleavage product) in Figure 3B emerged after 20-min incubation and increased gradually. On the other hand, band 8 (probable first cleavage product) in Figure S1B was detected faintly after 30-min incubation but increased quite slowly (see Additional file 1: Figures S1B and S1D). Band 9 in Figure S1C was also detected in a similar manner as band 8 (see Additional file 1: Figure S1C). Our results indicated that longer 5' overhangs with stable stem structures could reduce the efficiency or rate of substrate cleavage.

Processing of an endogenous hairpin RNA with 5' overhangs, pre-mmu-mir-1982 RNA, by recombinant DICER protein

To demonstrate the processing ability of DICER protein with not only designed pre-miRNA with 5' overhangs but natural pre-miRNA with 5' overhangs, we performed the processing experiment using pre-mmu-mir-1982 RNA with rDICER. The cleavage products were detected by Northern blotting using two different probes, probe-4 and probe-5, corresponding to antisense sequences of bases 12-31 and bases 52-74 of pre-mmu-mir-1982 RNA, respectively (see Figure 6A). Using probe-4, band 5 (~35 nt) appeared after 10 min incubation and gradually increased. After 40 min incubation, band 6 (~23 nt) was detected and the abundance of band 6 increased in a time-dependent manner (see Figure 6B). Additionally, using probe-5, band 7 (~23 nt) was detected from the 10-min incubation sample (see Figure 6C). Pre-mmu-mir-1982 RNA can also be processed by *in vitro* rDICER activity.

To analyze that band 5 could be further processed to band 6, we labelled the 5' end of the pre-mmu-mir-1982 RNA and incubated the samples with rDICER for 0, 2 and 16 hours (see Figure 7A). The signal intensity of 35-nt band decreased in a time-dependent manner, while on the other hand, the 12-nt band increased (see Figures 7B and 7C). These results showed that band 5 was a 35-nt product of initial rDICER processing and 12 nt from the 5'end were eliminated by a second, rDICER-catalyzed cleavage reaction generating a 23-nt product. Our results indicated that mature miR-1982 and miR-1982* RNA could be generated *in vitro* from pre-mmu-mir-1982 RNA by the two-step DICER processing reaction described above.

In addition to miRNA maturation, mammalian DICER also processes other kinds of small RNAs including endo-siRNAs [33,37-39]. It has been reported that mammalian endo-siRNAs are processed from various precursors including long hairpin RNAs and naturally formed dsRNAs resulting from bidirectional transcripts or antisense transcripts from pseudogenes. Although the complete structure of these precursor

Figure 4 Two-step processing of the 5'-end labelled RNA-I by recombinant DICER protein. (**A**) *In vitro* processing of the 5'-end labelled RNA-I by rDICER protein. 5'-end labelled RNA-I RNAs were incubated without rDICER for 120 min (lane 1) and with rDICER for the following time points (0, 10, 20, 30, 40, 50, 60 and 120 min; lane 2-9 respectively). The processing reaction was faster than the results of Figure 3B because the amount of RNA substrate in this reaction mixture was less. The RNA products less than 10 nt look stacked at the end of the gel because of the difficulty in separating efficiently, even at 7.5 M urea denaturing 20% polyacrylamide sequence gel. This experiment was repeated and replicated consistently. M: decade marker. (**B**) Sequences of band 1 and 2 in Figure 3B identified from Figure 4A and Table 1. Sequences highlighted in gray are 29-nt (band 1) and 23-nt RNA (band 2) from the 5' strand, respectively.

dsRNAs remains unclear, it seems likely that they have diverse 5' and 3' structures. Our results indicate DICER tolerance for 5' substrate overhang, potentially increasing the range of small RNA substrates that DICER can process. Recently, it was reported that the AGO2 protein could bind not only siRNAs and miRNAs but longer RNAs and pre-miRNAs [22,40]. However, most endogenous AGO2 proteins bind miRNAs [41] and the RISC requires 3' overhangs for the dsRNA incorporation [3,42]. As this research shows, DICER could process pre-miRNAs, longer dsRNAs and hairpin RNAs with 5' overhangs into dsRNA with 3' overhangs, which might be subsequently loaded with canonical length to the RISC. Further experimentation is required to connect our findings with the AGO loading mechanism.

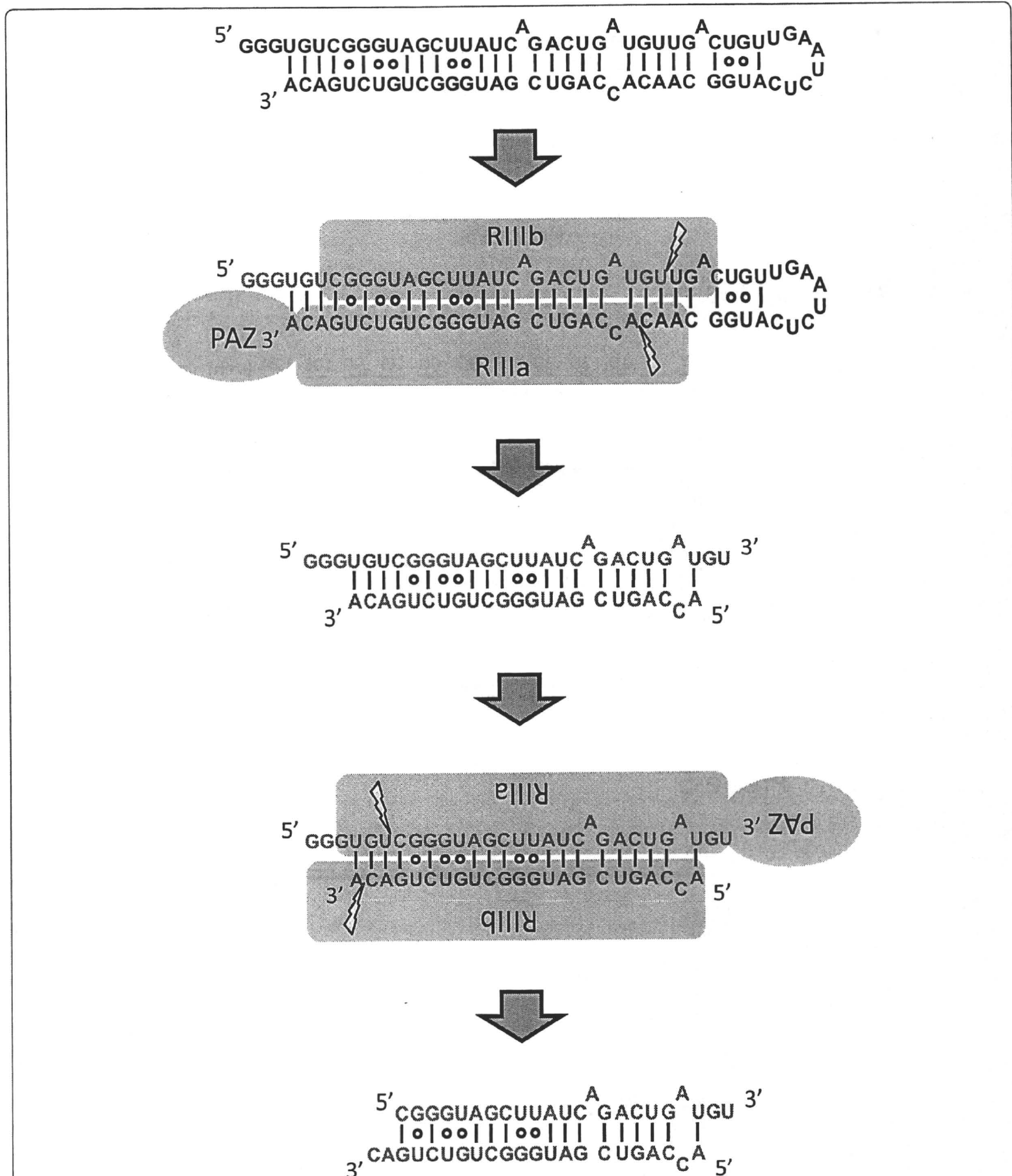

Figure 5 Model of the two-step processing of hairpin RNA with 5' overhangs (RNA-I) by DICER protein. rDICER processes hairpin RNA with 5' overhangs (RNA-I) to dsRNA with 29 nt-5' strand and 23 nt-3' strand after the first cleavage reaction and releases once from the binding site. Then, the dsRNA is bound in the inverse direction with the same or different rDICER molecule and is measured after the anchoring 3' end of the 29-nt strand to generate dsRNA with 23 nt cleaved from the 29-nt strand and 22 nt cleaved from the 23-nt strand. "PAZ" domain of rDICER colored purple; "RIIIa" and "RIIIb" domain of rDICER colored blue. Lightning marks indicate the cleavage sites in the RNA.

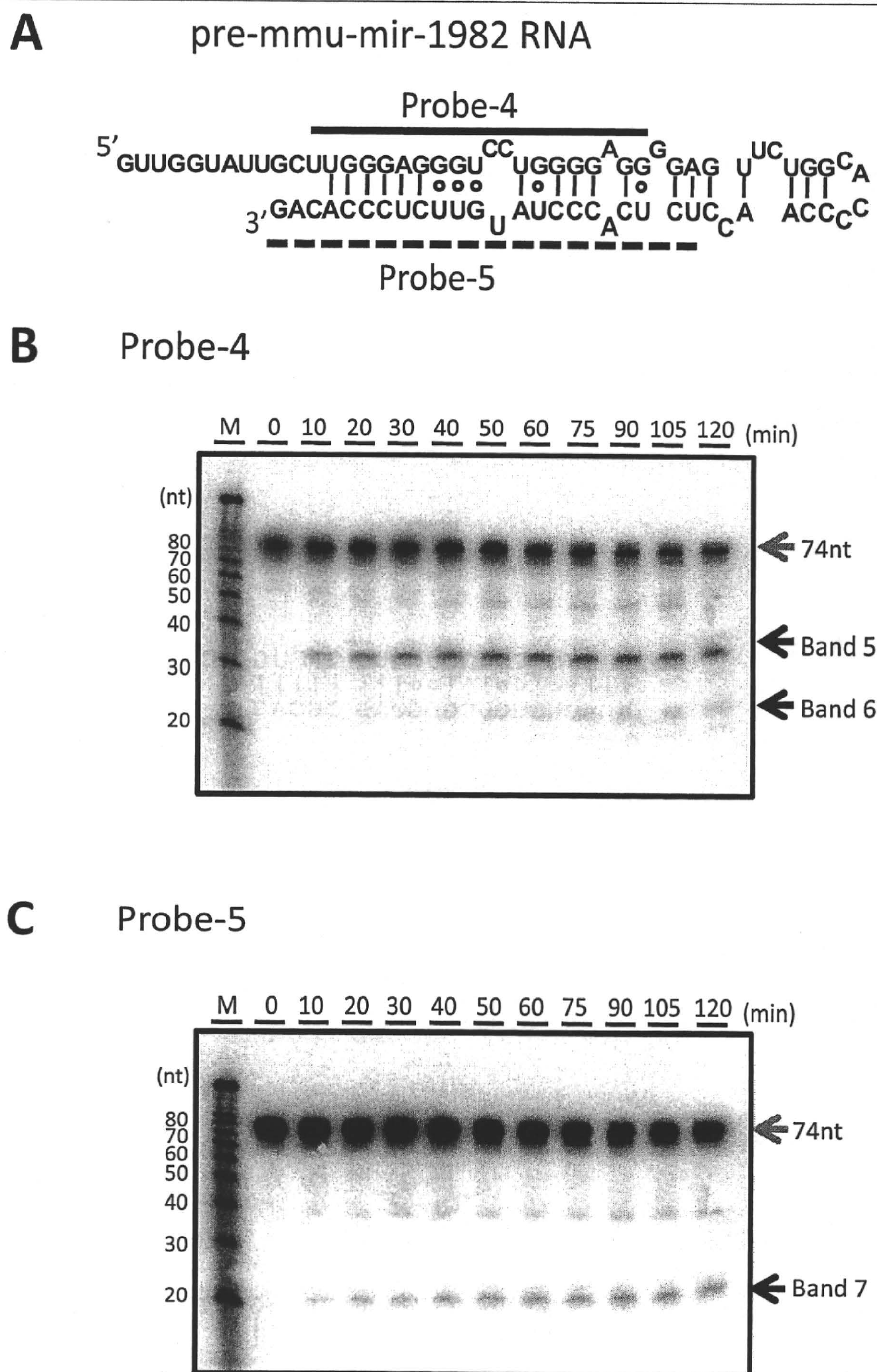

Figure 6 Processing of pre-mmu-mir-1982 RNA by recombinant DICER protein. (**A**) Pre-mmu-mir-1982 RNA and probes used in this study. The secondary structure was predicted using the CentroidFold program [49]. The solid line shows the position of probe-4 and the dashed line shows the position of probe-5. (**B-C**) Time-course analysis of the processing of pre-mmu-mir-1982 RNA by the rDICER protein. pre-mmu-mir-1982 RNAs were incubated with rDICER *in vitro* for the indicated time points (0, 10, 20, 30, 40, 50, 60, 75, 90, 105 and 120 min). The RNAs processed by rDICER were detected using probe-4 (**B**), probe-5 (**C**) by Northern blotting. The gray arrow shows the band of unprocessed RNA and the black arrow shows the bands of small RNA processed from the 5′ strand and 3′ strand of pre-mmu-mir-1982 RNA respectively. M: decade marker.

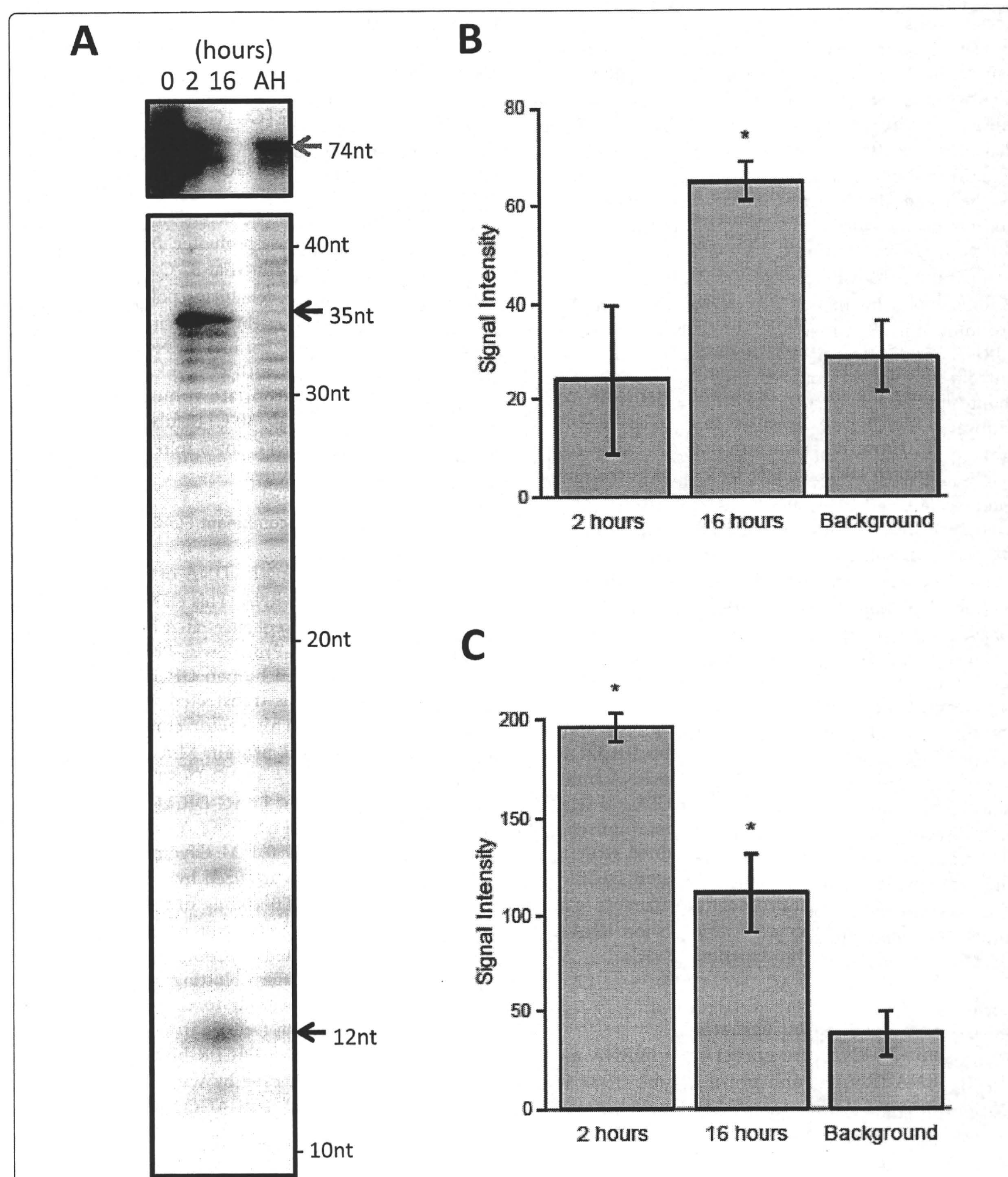

Figure 7 Two-step processing of the 5'-end labelled pre-mmu-mir-1982 RNA by recombinant DICER protein. (**A**) *In vitro* processing of the pre-mmu-mir-1982 RNA by the rDICER protein at a longer incubation time. 5' labelled pre-mmu-mir-1982 RNAs were incubated with rDICER for 0, 2 and 16 hours. The gray arrow shows the band of unprocessed RNA and the black arrow shows the bands of small RNA processed from pre-mmu-mir-1982 RNA. AH: the alkaline hydrolysis ladder of pre-mmu-mir-1982 RNA. The size of each band was determined by the AH ladder. (**B-C**) The signal intensities were quantified from the 12 nt (**B**) and 35 nt (**C**) bands in Figure 7A. These plots show average values bracketed by s.e.m. error bars; calculated from two independent experiments. Background refers to the signal intensity of the same sized band in the AH lane. The p-value was calculated using a simple t-test for each time point (2 hrs and 16 hrs) relative to the background. Significant differences ($p < 0.05$) in signal intensities are denoted with an asterisk. The significant calculated p-values are as follows: the 12-nt band at 16 hours, $p = 0.017$; the 35-nt band at 2 hours, $p = 0.0073$; and the 35-nt band at 16 hours, $p = 0.024$.

Conclusions

We show human rDICER recognizes and processes a hairpin RNA bearing a trinucleotide-5' overhang, and the two-step cleavage by rDICER forms canonical miRNA duplexes from the hairpin RNAs. It indicates that human rDICER functions as a molecular ruler by anchoring the 3' end of both the hairpin RNA with 5' overhangs and the 5' strand in the intermediate duplex. Moreover, an endogenously-expressed pre-miRNA with 5' overhangs, pre-mmu-mir-1982, also can be utilized as a substrate of rDICER and processed into a canonical miRNA duplex by the two-step cleavage reaction. While pre-mmu-mir-1982 RNA is a naturally expressed pre-miRNA [33,35], this 5'-overhanged structure is not a suitable substrate for nuclear export by Exportin-5 [43] and, assuming the absence of possible alternative export pathways, may not be presented to cytoplasmic DICER in the cells. However, it is worth noting a recent report, that mammalian DICER might be located in the nucleus and associate with ribosomal DNA chromatin [44]. We have also observed human DICER localized in both cytoplasm and nucleus (unpublished data, Ando *et al.*). These findings raise the intriguing possibility that nuclear DICER could process hairpin RNA with 5'-overhangs, like pre-mmu-mir-1982 RNA.

The two-step cleavage of a hairpin RNA with 5' overhangs shows that rDICER can release dsRNAs after the first cleavage and binds them again in the inverse direction for a second cleavage. The DICER protein's ability to release and bind dsRNA again indicates DICER could be capable of binding and processing dsRNA multiple times during short RNA maturation. DICER has recently been linked to the processing of diverse non-coding RNA precursors with as-yet undetermined structures. The experiments performed above suggest DICER has considerable flexibility in processing precursors, contributing to an ability to generate various short RNA products for incorporation into functional RISCs.

Methods

Preparation of hairpin RNA substrates

Pre-hsa-mir-21 RNA (pre-mir-21), pre-miRNA mimic hairpin RNA (RNA-I) and pre-mmu-mir-1982 RNA used in this study were generated by *in vitro* transcription using the Ampliscribe T7 High Yield Transcription kits (Epicentre) according to manufacturer's instructions. We made double-stranded DNA templates with T7 RNA polymerase promoter sequence by overlap-PCR using the following oligonucleotide pair; pre-mir-21-sense 5'-taatacgactcactatagAGCTTATCAGACTGATGTTGACTG-3' and pre-mir-21-antisense 5'-ACAGCCCATCGACTGGTGTTGCCATGAGATTCAACAGTCAACATC-3', RNAI-sense 5'-taatacgactcactatagggTGTCGGGTAGCTTATCAGACTGATGTTGA-3' and RNAI-antisense 5'-TGTCAGACAGCCCATCGACTGGTGTTGCCATGAGATTCAACAGTCAACA-3', pre-mmu-mir-1982-sense 5'-taatacgactcactataGTTGGTATTGCTTGGGAGGGTCCTGGGGAGGGGAGTT-3' and pre-mmu-mir-1982-antisense 5'-CTGTGGGAGAACATAGGGTGAGAGGTTGGGGTGCCAGAACTCCCCTCCCCA-3'. The overlapped sequences are underlined and the lower-case characters show the sequence of the T7 RNA polymerase promoter. *In vitro* transcription reactions were performed at 37°C overnight. Transcripts were run on 10% denaturing polyacrylamide gels in 0.5x TBE (45 mM Tris-borate, 1 mM EDTA), gel-excised, eluted from the gel in 1 M NaCl at 4°C overnight, and precipitated with ethanol. The pellet was resuspended in an appropriate volume of water and stored into the freezer at -30°C. Before use, RNA substrates were heated to 70°C for 5 min and then slowly cooled to room temperature.

Affinity purification of recombinant FLAG-DICER fusion proteins

We assembled a full-length cDNA of human DICER1 protein from HeLa total RNA. This cDNA sequence was identical to the coding sequence cited in the Swiss-Prot Protein Database (Swiss-Prot) [Swiss-Prot: Q9UPY3]. N-terminally FLAG-tagged human DICER1 protein was purified from 293T cells transfected with the plasmid pCA-FLAG-DICER1. This vector contained the full-length human DICER1 protein FLAG-tagged at the amino terminus in a pCA-FLAG-DEST vector [45]. We purified the recombinant FLAG-DICER1 fusion protein (rDICER) using ANTI-FLAG M2-Agarose Affinity Gel (Sigma) and eluted by 0.1 M Glycine-HCl (pH3.5). Then, the eluate was neutralized by Tris-HCl (pH8.0). The average yield was 50-100 μg of the active form of rDICER protein from 1×10^8 culture cell. Purified rDICER protein was detected by Coomassie Brilliant Blue (CBB) staining and Western blotting using anti-DICER (H212, Santa Cruz) antibody to check for successful homogenous purification (see Figures 1A and 1B). The contamination of known DICER-binding proteins in rDICER samples was checked by Western blotting using anti-FLAG (M2, Sigma), anti-AGO2 (07-590, Upstate) and anti-TRBP (ab42018, Abcam) antibody, respectively (see Figure 1C).

Processing of RNA substrates using recombinant DICER enzyme

The affinity-purified rDICER protein (2 pmol) was incubated with 45 pmol of RNA substrates (pre-mir-21 RNA, RNA-I or pre-mmu-mir-1982 RNA) in 1x reaction buffer (300 mM NaCl, 50 mM Tris-HCl, 20 mM

HEPES, 5 mM $MgCl_2$, pH 9.0) and 40 units of RNase-OUT (Invitrogen). These mixtures were incubated at 37°C for the indicated times. The reactions were purified by phenol-chloroform extraction followed by sodium acetate-ethanol precipitation at -20°C. The RNA pellet was resuspended in water at a final concentration of approximately 1 pmol/μl.

Northern blotting

rDICER-processed RNAs (1 pmol) were separated on 7 M urea-denaturing 20% polyacrylamide gels, then blotted onto Hybond-N+ membranes (GE Healthcare) using a Trans-Blot SD Semi-Dry Transfer Cell (Bio-Rad). Hybridization was performed in Church buffer (0.5 M $NaHPO_4$, pH 7.2, 1 mM EDTA and 7% SDS) containing 10^6 c.p.m./ml of each ^{32}P-labelled probe for 14 h. The membranes were washed in 2x SSC, and the signals were detected by autoradiography. All experiments were repeated and replicated consistently.

The probe sequences in this study were as follows: probe-1 (5'-TCAACATCAGTCTGATAAGCTA-3'), probe-2 (5'-ACAGCCCATCGACTGGTGTTG-3'), probe-3 (5'-CCATGAGATTCAACAG-3'), probe-4 (5'-CCTCCCCAGGACCCTCCCAA-3') and probe-5 (5'-CTGTGGGAGAACATAGGGTGAGA-3'). The probes were 5'-end labelled using T4 polynucleotide kinase (TaKaRa Bio) with [γ-^{32}P] ATP (6000Ci/mmol) at 37°C for 4 h.

Cloning of cleavage products

rDICER-processed RNAs (1 pmol) were separated on 7 M urea-denaturing 15% polyacrylamide gels, then the gel was stained by SYBR Gold (Invitrogen). The band around 23 nt was excised from the gel and purified as described above. The purified RNA was cloned by the Small RNA cloning kit (TaKaRa Bio) and sequenced by capillary sequencing.

5'-end labelling of the transcript

For the 5'-end labelling, RNA (45 pmol) was dephosphorylated with CIP at 37°C for 60 min. The reaction was inactivated by phenol-chloroform extraction and precipitated by sodium acetate-ethanol at -20°C. The pellet was resuspended in an appropriate volume of water. The dephosphorylated transcript was 5' end-labelled using T4 polynucleotide kinase (TaKaRa Bio) with [γ-^{32}P] ATP (3000Ci/mmol) at 37°C for 4 h. The 5'-end labeled transcript was PAGE-purified as described above and the RNA pellet was resuspended in water at a final concentration of approximately 0.5 pmol/μl. One microliter of this was used for the processing reaction by rDICER. These processed samples were run on 7.5 M urea-denaturing 20% polyacrylamide gels in 1x TBE buffer with RNA molecular marker or the products of alkaline hydrolysis of the same RNA molecule. The alkaline hydrolysis ladder was generated by incubating the labelled RNA in alkaline hydrolysis buffer (Ambion) at 100°C for 10 min. The signals were detected by autoradiography and quantified using ImageJ software (National Institutes of Health; http://rsb.info.nih.gov/ij/). The signal intensities were calculated as the mean of pixel value of selected area.

Additional material

Additional file 1: Supplementary information.

Acknowledgements
We thank Drs. Yasuhiro Tomaru, Timo Lassmann and Masanori Suzuki for their helpful discussion. We also thank Dr. Junichi Yano (Nippon Shinyaku Co. LTd., Kyoto) for the gift of materials. We acknowledge to RIKEN GeNAS for their support of our sequencing data production.
This work was supported by a Research Grant for the RIKEN Omics Science Center from the Ministry of Education, Culture, Sports, Science and Technology of Japan to YH.

Author details
[1]RIKEN Omics Science Center, 1-7-22 Suehiro-cho, Tsurumi-ku, Yokohama 230-0045, Japan. [2]Cancer Stem Cell Project, National Cancer Center Research Institute, 5-1-1 Tsukiji, Chuo-ku, Tokyo 104-0045, Japan. [3]Department of Biological Science and Technology, Tokyo University of Science, 2641 Yamazaki, Noda, Chiba 278-8510, Japan. [4]PREST, Japan Science and Technology Agency, 4-1-8 Honcho Kawaguchi, Saitama 332-0012, Japan.

Authors' contributions
YA conceived the study, designed and performed experiments and drafted the manuscript. YM and AM participated in the experimental design and performed experiments. RK and JC participated in the experimental design and purified recombinant FLAG-DICER fusion proteins. AMB, HS and KM participated in the design of the study and revised the manuscript. YH designed the research project, provided funding, supervised the study and critically reviewed the manuscript. All authors read and approved the final manuscript.

Received: 21 June 2010 Accepted: 9 February 2011
Published: 9 February 2011

References

1. Sontheimer EJ: **Assembly and function of RNA silencing complexes.** *Nat Rev Mol Cell Biol* 2005, **6(2)**:127-138.
2. Kim VN, Han J, Siomi MC: **Biogenesis of small RNAs in animals.** *Nat Rev Mol Cell Biol* 2009, **10(2)**:126-139.
3. Jinek M, Doudna JA: **A three-dimensional view of the molecular machinery of RNA interference.** *Nature* 2009, **457(7228)**:405-412.
4. Denli AM, Tops BB, Plasterk RH, Ketting RF, Hannon GJ: **Processing of primary microRNAs by the Microprocessor complex.** *Nature* 2004, **432(7014)**:231-235.
5. Gregory RI, Yan KP, Amuthan G, Chendrimada T, Doratotaj B, Cooch N, Shiekhattar R: **The Microprocessor complex mediates the genesis of microRNAs.** *Nature* 2004, **432(7014)**:235-240.
6. Han J, Lee Y, Yeom KH, Nam JW, Heo I, Rhee JK, Sohn SY, Cho Y, Zhang BT, Kim VN: **Molecular basis for the recognition of primary microRNAs by the Drosha-DGCR8 complex.** *Cell* 2006, **125(5)**:887-901.
7. Lund E, Guttinger S, Calado A, Dahlberg JE, Kutay U: **Nuclear export of microRNA precursors.** *Science* 2004, **303(5654)**:95-98.
8. Gregory RI, Chendrimada TP, Cooch N, Shiekhattar R: **Human RISC couples microRNA biogenesis and posttranscriptional gene silencing.** *Cell* 2005, **123(4)**:631-640.

9. Lee Y, Hur I, Park SY, Kim YK, Suh MR, Kim VN: **The role of PACT in the RNA silencing pathway.** *EMBO J* 2006, **25(3)**:522-532.
10. MacRae IJ, Ma E, Zhou M, Robinson CV, Doudna JA: **In vitro reconstitution of the human RISC-loading complex.** *Proc Natl Acad Sci USA* 2008, **105(2)**:512-517.
11. Tahbaz N, Kolb FA, Zhang H, Jaronczyk K, Filipowicz W, Hobman TC: **Characterization of the interactions between mammalian PAZ PIWI domain proteins and Dicer.** *EMBO Rep* 2004, **5(2)**:189-194.
12. Schwarz DS, Hutvagner G, Du T, Xu Z, Aronin N, Zamore PD: **Asymmetry in the assembly of the RNAi enzyme complex.** *Cell* 2003, **115(2)**:199-208.
13. Winter J, Jung S, Keller S, Gregory RI, Diederichs S: **Many roads to maturity: microRNA biogenesis pathways and their regulation.** *Nat Cell Biol* 2009, **11(3)**:228-234.
14. Khvorova A, Reynolds A, Jayasena SD: **Functional siRNAs and miRNAs exhibit strand bias.** *Cell* 2003, **115(2)**:209-216.
15. Yoda M, Kawamata T, Paroo Z, Ye X, Iwasaki S, Liu Q, Tomari Y: **ATP-dependent human RISC assembly pathways.** *Nat Struct Mol Biol* 2010, **17(1)**:17-23.
16. Tomari Y, Matranga C, Haley B, Martinez N, Zamore PD: **A protein sensor for siRNA asymmetry.** *Science* 2004, **306(5700)**:1377-1380.
17. Tomari Y, Du T, Zamore PD: **Sorting of Drosophila small silencing RNAs.** *Cell* 2007, **130(2)**:299-308.
18. Wang HW, Noland C, Siridechadilok B, Taylor DW, Ma E, Felderer K, Doudna JA, Nogales E: **Structural insights into RNA processing by the human RISC-loading complex.** *Nat Struct Mol Biol* 2009, **16(11)**:1148-1153.
19. Tomari Y, Zamore PD: **Perspective: machines for RNAi.** *Genes Dev* 2005, **19(5)**:517-529.
20. Hu HY, Yan Z, Xu Y, Hu H, Menzel C, Zhou YH, Chen W, Khaitovich P: **Sequence features associated with microRNA strand selection in humans and flies.** *BMC Genomics* 2009, **10**:413.
21. Burroughs AM, Ando Y, de Hoon MJ, Tomaru Y, Nishibu T, Ukekawa R, Funakoshi T, Kurokawa T, Suzuki H, Hayashizaki Y, *et al*: **A comprehensive survey of 3' animal miRNA modification events and a possible role for 3' adenylation in modulating miRNA targeting effectiveness.** *Genome Res* 2010, **20(10)**:1398-1410.
22. Tan GS, Garchow BG, Liu X, Yeung J, Morris JPt, Cuellar TL, McManus MT, Kiriakidou M: **Expanded RNA-binding activities of mammalian Argonaute 2.** *Nucleic Acids Res* 2009, **37(22)**:7533-7545.
23. Sakurai K, Amarzguioui M, Kim DH, Alluin J, Heale B, Song MS, Gatignol A, Behlke MA, Rossi JJ: **A role for human Dicer in pre-RISC loading of siRNAs.** *Nucleic Acids Res* 2010.
24. MacRae IJ, Doudna JA: **Ribonuclease revisited: structural insights into ribonuclease III family enzymes.** *Curr Opin Struct Biol* 2007, **17(1)**:138-145.
25. Zhang H, Kolb FA, Jaskiewicz L, Westhof E, Filipowicz W: **Single processing center models for human Dicer and bacterial RNase III.** *Cell* 2004, **118(1)**:57-68.
26. Macrae IJ, Zhou K, Li F, Repic A, Brooks AN, Cande WZ, Adams PD, Doudna JA: **Structural basis for double-stranded RNA processing by Dicer.** *Science* 2006, **311(5758)**:195-198.
27. MacRae IJ, Zhou K, Doudna JA: **Structural determinants of RNA recognition and cleavage by Dicer.** *Nat Struct Mol Biol* 2007, **14(10)**:934-940.
28. Zhang H, Kolb FA, Brondani V, Billy E, Filipowicz W: **Human Dicer preferentially cleaves dsRNAs at their termini without a requirement for ATP.** *EMBO J* 2002, **21(21)**:5875-5885.
29. Flores-Jasso CF, Arenas-Huertero C, Reyes JL, Contreras-Cubas C, Covarrubias A, Vaca L: **First step in pre-miRNAs processing by human Dicer.** *Acta Pharmacol Sin* 2009, **30(8)**:1177-1185.
30. Ruby JG, Jan CH, Bartel DP: **Intronic microRNA precursors that bypass Drosha processing.** *Nature* 2007, **448(7149)**:83-86.
31. Okamura K, Hagen JW, Duan H, Tyler DM, Lai EC: **The mirtron pathway generates microRNA-class regulatory RNAs in Drosophila.** *Cell* 2007, **130(1)**:89-100.
32. Berezikov E, Chung WJ, Willis J, Cuppen E, Lai EC: **Mammalian mirtron genes.** *Mol Cell* 2007, **28(2)**:328-336.
33. Babiarz JE, Ruby JG, Wang Y, Bartel DP, Blelloch R: **Mouse ES cells express endogenous shRNAs, siRNAs, and other Microprocessor-independent, Dicer-dependent small RNAs.** *Genes Dev* 2008, **22(20)**:2773-2785.
34. Glazov EA, Kongsuwan K, Assavalapsakul W, Horwood PF, Mitter N, Mahony TJ: **Repertoire of bovine miRNA and miRNA-like small regulatory RNAs expressed upon viral infection.** *PLoS One* 2009, **4(7)**:e6349.
35. Chiang HR, Schoenfeld LW, Ruby JG, Auyeung VC, Spies N, Baek D, Johnston WK, Russ C, Luo S, Babiarz JE, *et al*: **Mammalian microRNAs: experimental evaluation of novel and previously annotated genes.** *Genes Dev* 2010, **24(10)**:992-1009.
36. Starega-Roslan J, Krol J, Koscianska E, Kozlowski P, Szlachcic WJ, Sobczak K, Krzyzosiak WJ: **Structural basis of microRNA length variety.** *Nucleic Acids Res* 2011, **39(1)**:257-268.
37. Tam OH, Aravin AA, Stein P, Girard A, Murchison EP, Cheloufi S, Hodges E, Anger M, Sachidanandam R, Schultz RM, *et al*: **Pseudogene-derived small interfering RNAs regulate gene expression in mouse oocytes.** *Nature* 2008, **453(7194)**:534-538.
38. Watanabe T, Totoki Y, Toyoda A, Kaneda M, Kuramochi-Miyagawa S, Obata Y, Chiba H, Kohara Y, Kono T, Nakano T, *et al*: **Endogenous siRNAs from naturally formed dsRNAs regulate transcripts in mouse oocytes.** *Nature* 2008, **453(7194)**:539-543.
39. Maida Y, Yasukawa M, Furuuchi M, Lassmann T, Possemato R, Okamoto N, Kasim V, Hayashizaki Y, Hahn WC, Masutomi K: **An RNA-dependent RNA polymerase formed by TERT and the RMRP RNA.** *Nature* 2009, **461(7261)**:230-235.
40. Burroughs AM, Ando Y, Hoon ML, Tomaru Y, Suzuki H, Hayashizaki Y, Daub CO: **Deep-sequencing of human Argonaute-associated small RNAs provides insight into miRNA sorting and reveals Argonaute association with RNA fragments of diverse origin.** *RNA Biol* 2011.
41. Azuma-Mukai A, Oguri H, Mituyama T, Qian ZR, Asai K, Siomi H, Siomi MC: **Characterization of endogenous human Argonautes and their miRNA partners in RNA silencing.** *Proc Natl Acad Sci USA* 2008, **105(23)**:7964-7969.
42. Elbashir SM, Martinez J, Patkaniowska A, Lendeckel W, Tuschl T: **Functional anatomy of siRNAs for mediating efficient RNAi in Drosophila melanogaster embryo lysate.** *EMBO J* 2001, **20(23)**:6877-6888.
43. Okada C, Yamashita E, Lee SJ, Shibata S, Katahira J, Nakagawa A, Yoneda Y, Tsukihara T: **A high-resolution structure of the pre-microRNA nuclear export machinery.** *Science* 2009, **326(5957)**:1275-1279.
44. Sinkkonen L, Hugenschmidt T, Filipowicz W, Svoboda P: **Dicer is associated with ribosomal DNA chromatin in mammalian cells.** *PLoS One* 2010, **5(8)**: e12175.
45. Kimura R, Yoda A, Hayashizaki Y, Chiba J: **Novel ELISA using intracellularly biotinylated antigen for detection of antibody following DNA immunization.** *Jpn J Infect Dis* 2010, **63(1)**:41-48.
46. Griffiths-Jones S: **The microRNA Registry.** *Nucleic Acids Res* 2004, , **32 Database**: D109-111.
47. Griffiths-Jones S, Grocock RJ, van Dongen S, Bateman A, Enright AJ: **miRBase: microRNA sequences, targets and gene nomenclature.** *Nucleic Acids Res* 2006, , **34 Database**: D140-144.
48. Griffiths-Jones S, Saini HK, van Dongen S, Enright AJ: **miRBase: tools for microRNA genomics.** *Nucleic Acids Res* 2008, , **36 Database**: D154-158.
49. Sato K, Hamada M, Asai K, Mituyama T: **CENTROIDFOLD: a web server for RNA secondary structure prediction.** *Nucleic Acids Res* 2009, , **37 Web Server**: W277-280.

doi:10.1186/1471-2199-12-6
Cite this article as: Ando *et al.*: Two-step cleavage of hairpin RNA with 5' overhangs by human DICER. *BMC Molecular Biology* 2011 12:6.

Submit your next manuscript to BioMed Central and take full advantage of:

- Convenient online submission
- Thorough peer review
- No space constraints or color figure charges
- Immediate publication on acceptance
- Inclusion in PubMed, CAS, Scopus and Google Scholar
- Research which is freely available for redistribution

Submit your manuscript at
www.biomedcentral.com/submit

BIOLOGICAL CHEMISTRY

Founded in 1877 by Felix Hoppe-Seyler as Zeitschrift für Physiologische Chemie

Felix Hoppe-Seyler (1825–1895) was a pioneer of biochemistry, remembered not only for his discovery of hemoglobin and his contributions to the chemical characterization of many other biological compounds and processes but also for having been the mentor of Friedrich Miescher and Albrecht Kossel. In his preface to the first issue of *Zeitschrift für Physiologische Chemie,* Felix Hoppe-Seyler coined the term *Biochemistry* ('Biochemie') for the then newly emerging discipline.

EDITOR-IN-CHIEF
H. Sies, Düsseldorf

EXECUTIVE EDITORS
F.U. Hartl, Martinsried
S. Ludwig, Münster
K. Sandhoff, Bonn
B. Turk, Ljubljana
A. Wittinghofer, Dortmund

ASSOCIATE EDITORS (GBM STUDY GROUPS)
C.-M. Becker, Erlangen
G. Böl, Berlin
R. Brandt, Osnabrück
R. Frank, Braunschweig
T. Friedrich, Freiburg
K. Giehl, Giessen
D. Heinz, Braunschweig
R. Horstkorte, Halle/Saale
D. Klostermeier, Basel
I. Koch, Frankfurt/Main
P. Rehling, Göttingen
T. Roitsch, Würzburg
S. Schuchardt, Hannover
C. Seidel, Düsseldorf
R. Sterner, Regensburg
R. Tampé, Frankfurt/Main

EDITORIAL BOARD
W. Baumeister, Martinsried
B. Brüne, Frankfurt/Main
A. Bürkle, Konstanz
E. Cadenas, Los Angeles
I. Dikic, Frankfurt/Main
H. Fritz, Munich
C. Hammann, Darmstadt
D. Häussinger, Düsseldorf
L.-O. Klotz, Edmonton
A. Krüger, Munich
V. Magdolen, Munich
M. Müschen, Los Angeles
M. Naumann, Magdeburg
G. Pejler, Uppsala
N. Pfanner, Freiburg
R. Pike, Melbourne
J. Potempa, Krakow
P. Saftig, Kiel
W. Schaffner, Zürich
I. Sinning, Heidelberg
C. Sommerhoff, Munich

Biological Chemistry is associated with the Gesellschaft für Biochemie und Molekularbiologie e.V. (GBM)

DE GRUYTER

Biol. Chem., Vol. 392, pp. 299–304, April 2011 • Copyright © by Walter de Gruyter • Berlin • New York. DOI 10.1515/BC.2011.035

Minireview

RNA-dependent RNA polymerases in RNA silencing

Yoshiko Maida[1] and Kenkichi Masutomi[1,2,*]

[1]Division of Cancer Stem Cell, National Cancer Center Research Institute, 5-1-1 Tsukiji, Chuo-ku, Tokyo 104-0045, Japan
[2]PREST, Japan Science and Technology Agency, 4-1-8 Honcho Kawaguchi, Saitama 332-0012, Japan

* Corresponding author
e-mail: kmasutom@ncc.go.jp

Abstract

RNA-dependent RNA polymerases (RdRPs) synthesize double-stranded RNAs that are processed into small RNAs and mediate gene silencing. Viral RdRPs and cellular RdRPs show little structural homology to each other. Cellular RdRPs play key roles in RNA silencing by producing complementary strands for target RNAs via Dicer-dependent and -independent mechanisms. Although the existence of a functional mammalian homolog of RdRP has long been predicted, traditional approaches to identify such enzymes were unsuccessful. Recently, human telomerase reverse transcriptase, a polymerase closely related to viral RdRPs, has been shown to function as an RdRP and contributes to RNA silencing *in vivo*. These findings suggest that endogenous small interfering RNAs are produced by several mechanisms in eukaryotes.

Keywords: heterochromatin; human telomerase reverse transcriptase (hTERT); RNA component of mitochondrial RNA processing endoribonuclease (RMRP); RNA silencing; small interfering RNA (siRNA).

Introduction

RNA-dependent RNA polymerases (RdRPs) catalyze the formation of complementary RNA strands from single-stranded RNAs. In the beginning of evolution, all organisms used RNA as their genomes and RdRPs probably played pivotal roles for successive rounds of life cycle. RdRPs were identified from RNA viruses in the early 1960s (Baltimore et al., 1963), whereby RNA genomes encode viral RdRPs for the replication and transcription of their genomes. The discovery of eukaryotic RdRPs further revealed important functions of RdRPs *in vivo*. The first eukaryotic RdRP activity was found in Chinese cabbage in 1971 (Astier-Manifacier and Cornuet, 1971). Subsequently, the homologs were identified in other plants (Boege and Heinz, 1980), fungi (Cogoni and Macino, 1999) and nematodes (Smardon et al., 2000). These eukaryotic RdRPs are categorized as cellular RdRPs different from viral RdRPs, and the studies have revealed that cellular RdRPs play key roles in the regulation of gene expression through the RNA silencing mechanism.

The first report describing the RNA silencing phenomenon was published in 1928, before RNAs had been described. In the paper, Wingard described tobacco plants in which only the initially infected leaves were necrotic and diseased owing to tobacco ring spot virus, whereas the upper leaves had become asymptomatic and resistant to secondary infection, suggesting the acquisition of immunity to the virus (Wingard, 1928). This phenomenon was called 'recovery', and we now know that the 'recovery' from the virus disease involves RNA silencing (Covey et al., 1997). RNA silencing has been shown to be involved in various eukaryotic processes, such as defense against viruses and transposable elements, and developmental regulations. RNA silencing is a sequence-specific gene-regulatory mechanism, in which small RNAs, derived from precursor double-stranded RNAs (dsRNAs), repress the targeted gene expression transcriptionally and/or post-transcriptionally. In the organisms that possess RdRPs, the precursor dsRNAs are endogenously produced from the template single-stranded RNAs through the RdRP activity. In this review, we summarize the structural basis of RdRPs and the functions of RdRPs in gene regulation.

Structural and biochemical features of RdRP

There are two major groups of RdRP: viral RdRPs and cellular RdRPs. Viral and cellular RdRPs share little sequence homology. The crystal structures of viral RdRPs are similar to those of retroviral reverse transcriptases, and they share a structure resembling a closed 'right hand' containing palm, thumb and finger domains (Sousa, 1996). The palm domain structure is particularly conserved and contains four sequence motifs preserved in all of these polymerases, indicating the fundamental importance of these structural elements in the enzymatic function of the polymerases (van Dijk et al., 2004). The core of the 'palm' structure consists of two α-helices and a four-stranded antiparallel β-sheet, shared among numerous nucleic acids polymerases with RNA recognition motif.

Viral RdRPs initiate minus-strand RNA synthesis by two different mechanisms: *de novo* and primer-dependent initiation (van Dijk et al., 2004). *de novo* initiation, also known as primer-independent initiation, is widely used in RNA viruses for complete replication of viral genomes. Several RNA viruses initiate RNA synthesis using either nucleotide or uridylylated protein primers. The nucleotide primers used in primer-dependent initiation can be divided into two groups. One type is the orthodox primers binding to complementary

template RNA. This type of primer includes the oligonucleotide primers and the 5′ end of capped cellular mRNA (cap-snatched) primers. Another is the 3′ terminus of the template RNA that folds back as hairpin loop (back-priming). RNA viruses can use one or more priming mechanisms for RNA synthesis (van Dijk et al., 2004).

RdRPs are present in one or more copies in a wide range of eukaryotes, from early-branching parabasalids, such as *Giardia*, to multicellular forms, including plants, fungi, yeast and nematods (Table 1). These cellular RdRPs are encoded by *RDR* genes. Phylogenetic and protein motif analyses revealed a wide distribution of *RDR* homologs in eukaryote from protists to multicellular organisms, with no detectable prokaryotic or viral homologs (Zong et al., 2009). By contrast, no *RDR* homologs have been identified in vertebrate and insect genomes, even though these organisms also have RNA-mediated silencing mechanisms. Cellular RdRPs share the catalytic double-psi β-barrel (DPBB) domain, containing a signature metal-coordinating motif, with the universally conserved β′ subunit of DNA-dependent RNA polymerase (Salgado et al., 2006). For example, the RdRP of *Neurospora crasse*, QDE-1, has two DPBB motifs on a single polypeptide chain and it forms dimer for polymerase reaction (Salgado et al., 2006). The highly conserved region in the DPBB domain of cellular RdRPs includes the DbDGD motif (b is a bulky residue), and the similar DxDGD motif is conserved in the β′ subunit of DNA-dependent RNA polymerases. The DxDGD motif has been shown to be essential for cellular RdRP activity. Although the motif is reminiscent of the metal-binding GDD motif (motif C) of the viral RdRPs, each RdRP belongs to different superfamilies of nucleic acid polymerases, suggesting early branching of these polymerases in evolution. In principle, RDR proteins could mediate both primer-dependent and primer-independent RNA silencing (Sugiyama et al., 2005; Salgado et al., 2006). The primer-independent process can be seen in various organisms in the production of endogenous secondary small interfering RNAs (siRNAs) (Aoki et al., 2007), and the RNA products synthesized in this manner possess 5′-triphosphate termini, whereas siRNAs generated through the cleavage of long dsRNAs via RNase III enzymes share 5′-monophosphate structure (Aoki et al., 2007) (Figure 1A and B).

Roles of cellular RdRPs in RNA silencing

Cellular RdRPs play important roles in both transcriptional and post-transcriptional gene silencing (Figure 1). Plants have six *RDR*s (*RDR1–RDR6*) (Wassenegger and Krczal, 2006), and each of them is involved in different gene silencing mechanisms. *RDR1* and *RDR6* are induced upon the cellular defense against exogenous invaders, such as viruses, viriods and trangenes. Antiviral immunity in plants is conceptualized into three phases: initiation, amplification and systemic spread. In initiation, DICER-LIKE (DCL) proteins cleave dsRNAs of viral replicative products into primary siRNAs. Following initiation, RDR1 and RDR6 amplify the silencing signals via catalyzing the synthesis of new viral dsRNAs, which are processed into secondary viral siRNAs by DCLs. This RDR-dependent antiviral silencing resulted in more than 20-fold amplification of viral siRNAs (Wang et al., 2010). *RDR6* is also involved in post-transcriptional gene silencing. Post-transcriptional gene silencing is occasionally observed in plants carrying multiple copies of transgene constructs. Extensive primary transcription of trans-

Table 1 RNA-dependent RNA polymerases (RdRPs) in various organisms.

Organism	RdRP	Characteristic functions and products in gene silencing
Fungus		
Schizosaccharomyces pombe	Rdp1	PTGS, TGS
Neurospora crassa	QDE-1	PTGS, qiRNA
	Two others	
Plant		
Arabidopsis thaliana	RDR1	PTGS
	RDR2	TGS, RdDM
	RDR6	PTGS, ta-siRNA
	Three others	
Nematode		
Caenorhabditis elegans	EGO-1	PTGS, TGS, 22G-RNA
	RRF-1	PTGS, 22G-RNA
	RRF-3	PTGS, 26G-RNA
	One other	
Fruit fly		
Drosophila melanogaster	D-elp1	TGS
Mammal		
Homo sapiens	hTERT	PTGS

PTGS, post-transcriptional gene silencing; TGS, transcriptional gene silencing; qiRNA, QDE-2-interacting small RNA; RdDM, RNA-directed DNA methylation; ta-siRNA, *trans*-acting siRNA.

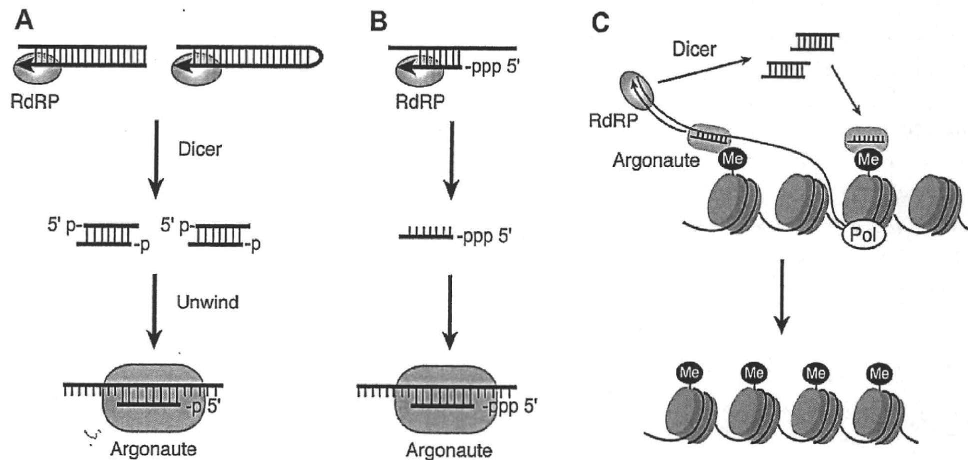

Figure 1 Common features of eukaryotic RdRP-dependent gene silencing pathways.
(A) Dicer-dependent functional small RNA synthesis. RdRPs produce long double-stranded RNAs, and the RNAs are cleaved into small double-stranded RNAs by Dicer. Argonautes load one of the strands for targeting. (B) Dicer-independent functional small RNA synthesis. RdRPs directly synthesize functional small RNAs *de novo*, independent of Dicer. (C) Heterochromatin formation. RdRPs produce antisense RNA strands for the transcripts from heterochromatic regions. Small RNAs from the regions guide histone H3K9 methylation.

genes leads to an accumulation of aberrant transgene mRNAs, which are decapped and/or unpolyadenylated (Luo and Chen, 2007). The aberrant RNAs are transcribed into dsRNA by RDR6, and subsequently processed into 21-bp siRNAs. The AGO1-bound siRNAs hybridize with complementary RNAs, both transgenes and related endogenous genes, thereby cleaving and downregulating the target RNAs. RDR6 amplifies post-transcriptional gene silencing through secondary dsRNA synthesis in a primer-dependent and primer-independent manner (Luo and Chen, 2007).

Transposable elements in eukaryotic genomes are typically silenced via the epigenetic mechanism. The plant *RDR2* genes are involved in the processes of RNA-dependent DNA methylation (RdDM) and RNAi-mediated heterochromatin formation. RdDM is triggered by the presence of nuclear dsRNAs, which are processed into 24-nt siRNAs via DCL3. The 24-nt siRNAs hybridize to the transcripts from methylated DNAs, and work as the guides for *de novo* methylation of DNA and histone H3K9 as well as RDR2-mediated secondary dsRNA production, which is required to maintain RdDM (Wassenegger and Krczal, 2006).

Plants have a unique class of endogenous siRNA named *trans*-acting siRNA (Allen et al., 2005; Cuperus et al., 2010). In *Arabidopsis*, the biogenesis of *trans*-acting siRNAs is initiated by miRNA-guided cleavage of *TAS* transcripts; *TAS1* and *TAS2* are cleaved by the AGO1-miR173 complex, *TAS3* is cleaved by the AGO7-miR390 complex, and *TAS4* is cleaved by the AGO1-miR828 complex. The resulting cleaved fragments are transformed into dsRNAs through primer-independent RNA synthesis of RDR6, and the dsRNAs are sequentially processed into phased *trans*-acting siRNA by DCL4. The miRNAs triggering biogenesis of *trans*-acting siRNAs are rather limited, and Cuperrus and co-workers recently reported that only miRNA in 22-nt length can contribute to the pathway, although most of the miRNAs in *Arabidopsis* are 21-nt (Cuperus et al., 2010).

Apart from plants with functionally different six RdRPs, non-plant eukaryotes encode fewer RdRPs and each RdRP manages more than one function of plant RdRPs. In the fission yeast *Schizosaccharomyces pombe*, a single homolog of plant RdRP (Rdp1) is associated with both RNAi and RNA-mediated heterochromatin formation (Wassenegger and Krczal, 2006). The centromeric repeats of the yeast genome form heterochromatin, whereas they are not completely silenced and transcribed by Pol II. The nascent transcripts from the centromeric region become the platforms for the RNA-induced transcriptional silencing (RITS) complex, which contains Ago1 loading the complementary siRNA. The RITS complex recruits RNA-dependent RNA polymerase complex (RDRC) containing Rdp1 to the centromere, and the RDRC promotes dsRNA synthesis from the transcripts, leading to the amplification of centromeric siRNAs. The RITS complex also recruits the Clr4-Rik1-Cul4 complex to the centromeric repeats, which mediates histone H3K9 methylation and heterochromatin formation (Sugiyama et al., 2005).

A filamentous fungus *Neurospora crassa* encodes an RdRP named QDE-1, which plays a key role in transgene-induced gene silencing (quelling) (Makeyev and Bamford, 2002). QDE-1 produces extensive RNA strands either in template-length or ~9–21-nt length (Makeyev and Bamford, 2002; Wassenegger and Krczal, 2006), which could contribute to Dicer-dependent or -independent silencing mechanisms, respectively. Recently, a new type of siRNA named QDE-2-interacting small RNA (qiRNA) was detected in *Neurospora*. The induction of qiRNA is triggered by DNA damage, and the RNA specifically corresponds to ribosomal DNA (rDNA). The production of qiRNA depends on QDE-1 and DCLs, suggesting precursor dsRNA formation through QDE-1, but RNA polymerase I, which is responsible for the transcription of rRNAs. Surprisingly, the precursor aberrant RNA of qiRNAs was transcribed from rDNA by QDE-1 itself through its DNA-dependent RNA polymerase activity,